

Accepted Manuscript

Title: Kinetics of the combustion of olive oil. A semi-global model

Author: Rafael Font María D. Rey María A. Garrido

PII: S0165-2370(14)00121-1

DOI: <http://dx.doi.org/doi:10.1016/j.jaap.2014.05.015>

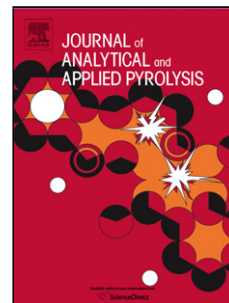
Reference: JAAP 3207

To appear in: *J. Anal. Appl. Pyrolysis*

Received date: 17-12-2013

Revised date: 14-3-2014

Accepted date: 12-5-2014



Please cite this article as: R. Font, M.D. Rey, M.A. Garrido, Kinetics of the combustion of olive oil. A semi-global model, *Journal of Analytical and Applied Pyrolysis* (2014), <http://dx.doi.org/10.1016/j.jaap.2014.05.015>

This is a PDF file of an unedited manuscript that has been accepted for publication. As a service to our customers we are providing this early version of the manuscript. The manuscript will undergo copyediting, typesetting, and review of the resulting proof before it is published in its final form. Please note that during the production process errors may be discovered which could affect the content, and all legal disclaimers that apply to the journal pertain.

1 Kinetics of the combustion of olive oil. A semi-global model

2 Rafael Font*, María D. Rey, María A. Garrido

3 Chemical Engineering Department, University of Alicante, P.O. Box 99, 03080

4 Alicante, Spain

5 1. INTRODUCTION

6 The increasing need of energy by segments of our society, the reduction of petroleum
7 reserves and increased environmental concerns have caused biomass materials to gain
8 much interest with respect to energy utilization. For example, waste vegetable oils can
9 through thermal decomposition be used to directly obtain energy or fuels [1]. It is very
10 important to perform thermal analysis of the oils to predict their behavior in real
11 combustion systems. The combustion kinetics of these fuels gives relevant information
12 on their thermal behavior and on the possible formation of a carbonaceous residue and
13 its subsequent oxidation.

14 Jansson et al. [2] studied the pyrolysis of olive oils and other vegetable oils, and
15 determined the evolved compounds on a Pyrolyzer/GC/MS. Gases such as propene and
16 liquids such as oleic acid, docosene and octadecenal, with boiling points at around 360
17 °C (633 K), were found. In a combustion process these compounds are oxidized, which
18 changes the composition of the gas phase.

19 The subject of a previous paper was a study of the pyrolysis kinetics of olive and used
20 olive oil [3]. The pyrolytic decomposition was analyzed taking into consideration the
21 vaporization process involved, and the results were compared with a number of kinetic
22 considerations discussed in other papers [4-6]. The proposed kinetic model considered
23 two sequential processes: a first process, considering vaporization and decomposition,
24 whose apparent activation energy and reaction order were 112 kJ/mol and 0.606,
25 respectively, and a second process, whose apparent activation energy and reaction order
26 were 194.6 kJ/mol and 2.274, respectively. The values obtained in both of these
27 processes are acceptable; in the first process, the values are between those of the

28 vaporization process and chemical decomposition, and in the second they were common
29 values for decomposition processes.

30 Others have also studied the oxidative thermal decomposition in order to characterize
31 vegetable oils [7,8]. Tran et al. [9] examined a number of mechanisms of the
32 combustion of oxygenated compounds of biofuels.

33 Dweck and Sampaio [10] analyzed the thermal decomposition of commercial vegetable
34 oils by TG/DTA and observed four decomposition steps. They proposed that the last
35 one corresponds to the burnout of the residual carbonaceous material.

36 Concerning the global kinetics, Vecchio et al. [7] studied the oxidative thermal
37 decomposition of single-varietal extra olive oil by TG/DSC, and observed a complex
38 multistep decomposition. They attributed the first apparent peak to two different
39 processes for the purpose of relating them to the chemical composition. From the first
40 decomposition step they obtained apparent activation energies for the de-convoluted
41 peaks ranging between 27 and 158 kJ/mol, and 31 and 278 kJ/mol for the first and
42 second peaks, respectively. No other information concerning kinetic parameters was
43 presented.

44 Gouveia de Souza et al. [11] elucidated the oxidation kinetics of sunflower oil by TG,
45 by considering three decomposition steps in which the interaction of the oxidation
46 reactions was important. The first step takes place between 503 and 653 K with reaction
47 order around 1 and activation energy around 90-110 kJ/mol, in which the volatile
48 compounds were removed by the vapor generated during heating. The second is
49 between 653 and 753 K with reaction order around 2 and activation energy of 205-300
50 kJ/mol. The third step takes place between 753 and 823 K and the deduced reaction
51 orders and apparent activation energies were around 2 and 300-400 kJ/mol,
52 respectively.

53 Santos et al. [12] considered three decomposition steps in the oxidative decomposition
54 of a number of edible oils, including olive oil. Similar kinetic parameters were obtained.
55 In the first step, the apparent activation energy was between 78 and 106 kJ/mol and the
56 reaction order was between 0.92 and 1.06. In the second step, the apparent activation
57 energy was between 208 and 349 kJ/mol and the reaction order was between 1.86 and
58 2.11. In the last step, an activation energy between 274 and 370 kJ/mol and a reaction

59 order between 1.87 and 2.13 were obtained. No values were reported for the mass
60 fractions of the volatiles evolved in each step.

61 Zhengwen [13] recently studied the combustion of cooking oil tar on a TG apparatus.
62 He observed four DTG peaks after the initial evaporation of the absorbed water, and
63 made several plots for correlating the data which suggest a model of First Order
64 Reaction and Three-dimensional Diffusion Separate-stage. However, values for the
65 apparent activation energy were not reported.

66 Vecchio et al. [14] studied the decomposition of triglycerides contained in olive oil by
67 TG. They observed the presence of four decomposition steps and determined the kinetic
68 parameters of the first two decomposition steps.

69 More recently, Tomassetti et al. [15] analyzed the thermal decomposition of saturated
70 mono-, di- and tri-glycerides. They also observed four decomposition steps and
71 proposed the kinetic parameters for the two or three first steps.

72 The decomposition kinetics of complex materials (synthetic polymers, biomass, oils,
73 etc.) is a subject that deals with the examination and analysis of kinetic parameters, with
74 a view to clarifying their significance [16-18]. Thus, efforts to study the decompositions
75 of substances such as vegetable oils can help to reduce the existing chaos in the field of
76 reaction kinetics of complex materials.

77 In this paper, a kinetic model for the combustion of olive oil at air atmosphere and also
78 in one that is oxygen-poor has been developed by simultaneous determination at each
79 step of the kinetic parameters and the mass fraction of the volatiles. The experimental
80 data are compared with those obtained by simulation using the deduced expressions. We
81 also discuss the possibility of a carbonaceous residue formed during the thermal
82 oxidation of the fuels in question, which has not been considered in previous papers.
83 The kinetic study is analyzed by contrasting with the study on olive oil by Vecchio et al.
84 [7], as well as other studies carried out on other vegetable oils. The kinetic model can be
85 used to characterize certain decomposition steps of the edible oils and/or their
86 corresponding wastes and to analyze the formation of a carbonaceous residue.

87

88 2. EXPERIMENTAL

89 2.1 Raw material

90 Pure olive oil, waste olive oil and waste mixed oil were selected as materials for
91 studying the kinetics. This study employed the same pure olive oil as a previous
92 pyrolysis kinetic study [3]. The waste olive oil was obtained after four/five frying
93 processes, which corresponds to an average use of this oil, and was also the same waste
94 olive oil employed in the previous pyrolysis kinetic study [3]. A waste mixed oil,
95 consisting of a mixture of different used cooking oils, was also utilized to determine
96 whether there are any great differences between the oils. An elemental analysis of the
97 samples was carried out on a Perkin-Elmer 2400 to determine the mass fractions of
98 carbon, hydrogen, nitrogen and sulphur; oxygen content was determined by a direct
99 oxygen analysis carried out on a Flash-2000 Thermo Fisher Scientific; a LECO
100 Instruments AC-350 calorimetric bomb was used to obtain the net calorific value. Table
101 1 shows the results of the elemental analysis and the net calorific values of the three
102 samples tested. As observed, there are no big differences between the samples.

103 Table 1

104 2.2 Apparatus and experimental procedure

105 The combustion runs at air atmosphere were carried out on two different TG apparatus
106 whereas in the $N_2:O_2 = 9:1$ runs only one of them was used:

107 1) A Mettler Toledo Thermobalance model TGA/SDTA851e/LF/1600. This instrument
108 incorporates a horizontal furnace and a parallel-guided balance. In this way, positioning
109 of the sample has no influence on the measurement, and flow gas perturbation and
110 thermal buoyancy are minimized. The sample temperature was measured by a sensor
111 directly attached to the sample holder. Two different atmospheres were used; $N_2:O_2 =$
112 $4:1$ and $N_2:O_2 = 9:1$. The crucibles employed in the runs were a nearly cylindrical
113 aluminum crucible of 0.55 cm internal diameter and 0.41 cm height, which is slightly
114 curved at the bottom of the cylinder, and a cylindrical alumina crucible of 0.47 cm
115 internal diameter and 0.42 cm height.

116 2) A Perkin Elmer Thermobalance model TGA/SDTA-6000. This instrument
117 incorporates a vertical furnace and a single beam vertical balance. As in the previous
118 case, positioning of the sample has no influence on the measurement, and flow gas
119 perturbation and thermal buoyancy are minimized. The SaTurnA sensor measures both

120 the sample and reference temperature directly for superb performance. The alumina
121 crucible used in all runs was nearly cylindrical with 0.65 cm internal diameter and 0.42
122 cm height and was slightly curved at the bottom of the cylinder. Synthetic air was used
123 as fluid, so these results can be compared with the results obtained at $N_2:O_2 = 4:1$ using
124 the Mettler Toledo Thermobalance.

125 Dynamic experiments were carried out at heating rates between 5 and 20 K/min, from
126 the initial room temperature up to 850 K, including thus the entire range of
127 decomposition. Isothermal experiments started at a constant heating rate until the
128 desired temperature was reached and then the final temperature was maintained
129 constant. The experiment was considered to have finished when the weight loss rate was
130 negligible (less than $1 \cdot 10^{-5} s^{-1}$). Small size samples, between 1 and 10 mg, were used in
131 the runs.

132 A pyrolysis run at a heating rate of 5 K/min using Avicel PH-105 microcrystalline
133 cellulose was done on each apparatus. The kinetic parameter values obtained showed
134 good agreement with the results reported by Grønli et al. [19] in their round-robin study
135 of cellulose pyrolysis kinetics by thermogravimetry (at 5 K/min and 244 kJ/mol, the
136 experimental and calculated data coincide, obtaining logarithmic values of the pre-
137 exponential factors of around 18.8, a value within the accepted interval). These
138 experiments were useful to check how well the two thermobalances performed.

139 The TG-MS runs were carried out on a Mettler Toledo model TG-ATD
140 TGA/SDTA851e/LF/1600 coupled to a ThermoStar GSD301T Pfeiffer Vacuum MS
141 apparatus using $He:O_2 = 4:1$ as carrier gas. The operating conditions were: a mass
142 sample of around 5 mg, a 30 K/min heating rate, a 70 eV ionization energy, and SIR
143 detection of several ions (4, 13-18, 25-32, 35-46 in one run and 4, 32, 43-46, 50-52, 55-
144 58, 60, 65, 68, 73, 78, 91, 96, 105, 106 in another run). The response of each ion was
145 divided by that of helium ($m/z=4$) and afterwards the corresponding minimum value
146 was subtracted from each response.

147 The TG-IR runs were carried out on a Perkin Elmer STA6000 and a Nicolet 6700 FT-IR
148 using air as carrier gas, a mass sample of around 12 mg and at 30 K/min heating rate.
149 The transmittance was measured between 4000 and $600 cm^{-1}$.

150 3. RESULTS AND DISCUSSION

151 Most of the TG runs were carried out on the Mettler Toledo Thermobalance in the
152 aluminium crucible. Figures 1 and 2 show the first experimental TG plots for the
153 combustion of pure olive oil, which must be analyzed in order to understand subsequent
154 runs and the proposed kinetic model. Figure 1a shows the TG runs carried out on the
155 Mettler Toledo (M-T) instrument for combustion and pyrolysis of pure olive oil (data
156 for the latter were obtained elsewhere [3]) at 10 K/min and for a 5 mg initial mass. As
157 observed, the thermal decomposition is faster under oxidative conditions. It is possible
158 that a carbonaceous residue has been formed by oxidation, whose subsequent
159 combustion results in the presence of a fraction in the oxidation run curve on the right
160 of the pyrolysis run curve. That this residue has been possibly formed should be
161 confirmed by means of other techniques, such as TG-MS and TG-IR, since other
162 explanations are also possible. Figure 1b shows the results of three runs carried out at 5,
163 10 and 20 K/min on an initial mass of 5 mg. It can be observed that the curves intersect,
164 which also occurs in other series of runs. The exothermal nature of the combustion run
165 can be confirmed from the variation in the temperature increment of the DTA
166 corresponding to 20 K/min, by noticing that there is an increase in temperature
167 throughout the entire process and a peak that coincides with the weight that has been
168 lost. Figure 1c shows the results of three TG runs carried out under the same operating
169 conditions but varying the initial masses. It can be seen that there is a considerable
170 difference between the experimental curves obtained for 1 and 5 mg on the one hand,
171 and 10 mg on the other. Concerning the experimental data, Figure 1d shows the results
172 of the TG (weight fraction) and DTG (mass fraction increment in volatiles per unit
173 temperature increment, $\Delta V/\Delta T$) for a run carried out at 5 K/min on 5 mg of oil. Three
174 peaks are visible at 600, 700 and 800 K (the label “cal” refers to data calculated by
175 means of the proposed model). The results of two other runs carried out under the same
176 operating conditions are shown in Figures 2a and 2b. Small differences between the
177 DTG curves can be observed, which demonstrates again that the runs are not exactly
178 reproducible. Figure 2c shows calculated results for the decomposition steps involved in
179 the reactions that are proposed in the following sections. Figure 2d shows the results of
180 a run carried out at 20 K/min on 5 mg of oil. In light of the previous results, the
181 following aspects deserve comment: a) at least three decomposition steps can be
182 considered based on the presence of three peaks in the DTG runs, b) the run carried out
183 on 10 mg has a curve that is very separated from the curves of the other two runs carried
184 out on 1 mg and 5 mg, probably as a consequence of the large sample mass, which

185 could cause the temperature of the samples to be different to that programmed (the
186 effect of sample mass must be considered to obtain acceptable results) c) there could be
187 a factor that leads to random behavior and provokes crossing of the curves. This can be
188 attributed to a vaporization process, as in the case of the pyrolysis runs [3]. Previous
189 studies have revealed that the vaporization processes exhibit a random variation in
190 weight loss vs. temperature in dynamic TG runs done within the interval of
191 vaporization, which is the result of irregular diffusion of vapours along the length of the
192 crucible [20,21]. No other reasons for the random behavior have been found.

193 Figures 1 and 2

194 Figure 3 shows the results of runs also carried out on the Mettler Toledo
195 Thermobalance, but now on 1 mg of pure olive oil. The DTA in Figure 3a is for the 20
196 K/min run and is indicative of an exothermic process throughout the entire run. The first
197 of the three peaks in the DTG plot in Figure 3c is very broad, so presumably four
198 decomposition steps, two decomposition steps corresponding to the broad peak and two
199 decomposition steps from the following two peaks should be considered when
200 analyzing the experimental data. Figures 3b and 3d show calculated data that will be
201 explained later.

202 Figure 3

203 The analysis of the runs carried out at $N_2:O_2 = 9:1$ atmosphere, the results of the runs
204 carried out with the Perkin Elmer Thermobalance and some results of the dynamic +
205 isothermal runs are presented in Supplementary Material.

206 Figures 4a to c show the TG curves of runs carried out on pure olive oil, waste olive oil
207 and waste mixed oil, respectively. The overall decomposition is similar in all cases in
208 spite of the thermal treatment undergone by the waste oils. Another TG run carried out
209 on waste olive oil at 10 K/min instead of 20 K/min is shown in Figure 4d.

210 Figure 4

211 Before turning to a description of the proposed kinetic model, the TG-MS and TG-IR
212 data will be presented and analyzed since they are useful in identifying the different
213 decomposition steps.

214 4. ANALYSIS OF TG-MS DATA

215 Figure 5 shows the results of the TG-MS run carried out on a 5 mg initial mass of pure
216 olive oil at 30 K/min and at a He:O₂ = 4:1 atmosphere (the high heating rate was
217 required to obtain acceptable signals for the evolved ions). The intensity of a number of
218 ions have been measured: water (18), carbon monoxide (28, including ethylene), carbon
219 dioxide (44) and methane (15). It can be seen that the ion corresponding to water
220 appears in the interval 500-750 K, coinciding with the thermal degradation of the olive
221 oil, except in the last step. By contrast, ions of both carbon oxides appear throughout the
222 entire decomposition process, from 500 to 850 K, indicating that the last decomposition
223 step corresponds to the combustion of a carbonaceous residue with formation of carbon
224 oxides and very little or no formation of water.

225 Considering the remaining TG-MS data, it seems that formaldehyde (ions 29 and 30),
226 acetaldehyde (ions 29 and 43), ethylene (ions 27 and 26, because ion 28 also
227 corresponds to carbon monoxide), acetylene (ions 26 and 25), other hydrocarbons (ions
228 25, 26, 27, 39, 40 41 and 42) and other oxygenated compounds (ion 57) are formed
229 inside the interval 500-750 K, including methane, as a consequence of the thermal
230 decomposition. The study has been extensive considering all the ions listed in the
231 experimental section. The emission of benzene, toluene or xylenes – ions 78, 91 or 106
232 – was not observed.

233 Figure 5
234

235 5. ANALYSIS OF THE TG-IR DATA

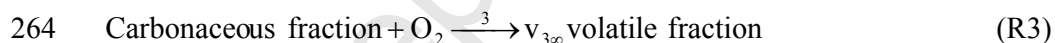
236 Figure 6 shows the results obtained in the dynamic run carried out on a 12 mg initial
237 mass of pure olive oil at 30 K/min in air, on the Perkin Elmer TG and the Nicolet FT-IR
238 apparatus. Figure 6a shows the transmittance at time 15.5 min, when the weight loss
239 rate is high. The following peaks have been identified in accordance with NIST data
240 base and Vlachos et al. [22]: 3400-4000 cm⁻¹ and 1300-1600 cm⁻¹ due to water vapor,
241 2300-2400 cm⁻¹ and 700 cm⁻¹ due to CO₂, 2100-2200 cm⁻¹ due to CO, 2850-3000 cm⁻¹
242 due to C-H bonds, 1700-1800 cm⁻¹ due to C-O bonds and 1150-1250 cm⁻¹ due to C-O
243 ester groups.

244 Figure 6

245 Figure 6b shows the variation of transmittance vs. time corresponding to a wavelength
 246 of 2930 cm^{-1} (C-H bond). Only one broad peak is observed. Similar trends occur in the
 247 case of the other wavelengths, except for those corresponding to CO and CO₂ (see
 248 Figure 9c where two broad peaks can be observed). This fact confirms the conclusion
 249 drawn based on the TG-MS results. The first broad peak in Figure 9c corresponds to
 250 decomposition reactions, whereas the second broad peak, only observed for CO₂ in
 251 Figure 6c and CO at its characteristic wavelength, correspond to the combustion of a
 252 carbonaceous residue accompanied by little or no formation of water and organic
 253 compounds. Similar trends were obtained in the case of the waste olive oil and waste
 254 mixed oil.

255 6. KINETIC MODEL

256 Several kinetic models were considered for the purpose of reproducing the experimental
 257 results. Since at least four decomposition steps must be taken into account, the
 258 following scheme of four parallel reactions has been proposed (reactions 1A and 1B
 259 corresponding to the first broad peak, reactions 2 and 3 for the following peaks in DTG
 260 runs):



265 where $v_{1A\infty}$, $v_{1B\infty}$, $v_{2\infty}$ and $v_{3\infty}$ are the maximum mass fractions of volatile products of
 266 reactions 1A, 1B, 2 and 3, respectively, having been produced long after the reactions
 267 had gone to completion. Taking into account that the final residue is negligible, the sum
 268 of these maximum mass fractions of volatiles must equal 1. The carbonaceous fraction
 269 in question is the one produced by any of the reactions 1A, 1B or 2.

270 This kinetic model is based on the decomposition steps observed and must be
 271 considered as a simplification of the complicated network of reactions that take place.
 272 This kinetic model must be considered as a correlation of the experimental data
 273 obtained.

274 For every reaction, the conversion degree is calculated as the ratio of the mass fraction
 275 of volatiles obtained at any instant during the reaction (V_i) to the corresponding yield
 276 coefficient or the mass fraction of volatiles at time infinity ($v_{i\infty}$), or

$$277 \quad \alpha_i = V_i / v_{i\infty} \quad i = 1A, 1B, 2 \text{ and } 3 \quad (1)$$

278 The kinetic equation of each reaction i can be expressed as

$$279 \quad d(V_i / v_{i\infty}) / dt = d\alpha_i / dt = k_i (1 - \alpha_i)^{n_i} = k_i (1 - (V_i / v_{i\infty}))^{n_i} \quad i = 1A, 1B, 2 \text{ and } 3 \quad (2)$$

280 For reaction 3, the same kinetic model is assumed to apply on the grounds that the
 281 carbonaceous residue is formed at low temperatures prior to combustion.

282 The kinetic constants are obtained from the Arrhenius equation, or

$$283 \quad k_i = k_{oi} \exp(-E_i / RT) \quad i = 1A, 1B, 2 \text{ and } 3 \quad (3)$$

284 By integrating the above equations, the conversion degrees can be calculated at every
 285 instant from a knowledge of the temperature program. The weight or mass fraction
 286 measured in the thermobalance (w) is related to the volatiles obtained (V) by:

$$287 \quad \begin{aligned} \text{Mass fraction} &= 1 - V = 1 - (V_{1A} + V_{1B} + V_2 + V_3) = \\ &= 1 - (v_{1A\infty} \alpha_{1A} + v_{1B\infty} \alpha_{1B} + v_{2\infty} \alpha_2 + v_{3\infty} \alpha_3) \end{aligned} \quad (4)$$

288 Assuming initial values for all the kinetic constants (k_{oi} , E_i , n_i) and maximum mass
 289 fractions, $v_{i\infty}$, we calculated the conversion degrees by integrating the differential
 290 equations in Eq. (2) above, using Euler's method and small time intervals, as well as
 291 optimization with the Solver function in an Excel spreadsheet. We subsequently
 292 checked that integration by Euler's method was accurate by decreasing the time
 293 interval, which gave the same results. It has also been confirmed that the kinetic
 294 parameters obtained by applying the iso-conversional method [23] to a reaction,
 295 coincide with those employed in the simulations using Euler's method, for small time
 296 intervals of the same order as those used in this work. The objective function (OF) to
 297 minimize was the sum of the square differences between the experimental and
 298 calculated mass fractions:

$$299 \quad OF = \sum_{m=1}^M \sum_{j=1}^N (\text{mass fraction}_{m,j}^{\text{exp}} - \text{mass fraction}_{m,j}^{\text{cal}})^2 \quad (5)$$

300 where M is the number of runs and N is the number of points in each run.

301 The validity of the model has been established by calculating the variation coefficient
302 (VC):

$$303 \quad VC = 100 \sqrt{(\overline{OF} / (N_{\text{total}} - P)) / \overline{\text{mass fraction}_{\text{exp}}}} \quad (6)$$

304 where N_{total} and P are the number of data values and parameters fitted, respectively, and
305 $\overline{\text{mass fraction}_{\text{exp}}}$ is the average mass fraction that remains inside the crucible, which is
306 close to 0.5. In accordance with the approach proposed in Martín-Gullón et al. [24], the
307 optimization was performed with respect to a ‘comparable kinetic constant’, K_i^* ,
308 instead of optimizing k_{oi} directly. This constant was calculated at a reference
309 temperature (T_{ref}) around the maximum decomposition rate, after the inclusion of a
310 factor $(0.64)^{n_i}$, as:

$$311 \quad K_i^* = k_i (0.64)^{n_i} = (k_{oi} \exp(-E_i / RT_{\text{ref}}))(0.64)^{n_i} \quad (7)$$

312 The number 0.64 was introduced to weaken the dependence of the reaction order and
313 the other kinetic parameters on each other [24]. From the optimized parameters K_i^* , E_i
314 and n_i , the values of k_{oi} can be deduced. Note that the parameter K_i^* is only used and
315 valid for correlation purposes, since it facilitates optimization and decreases the
316 computational time.

317 The optimization parameters for reactions 1A, 2 and 3 were K_i^* , E_i , n_i and $v_{i\infty}$. As for
318 reaction 1B, they were E_{1B} , n_{1B} , $v_{1B\infty}$ and the value of K_{1B}^* in each run. The fact that
319 K_{1B}^* varies between runs can be justified if a vaporization process takes place during the
320 devolatilization process; it has been established that the pre-exponential factor depends
321 on the initial mass in the vaporization process, and that it can vary between similar runs
322 due to a random process that depends on the heating rate [20,21].

323 To deduce the best kinetic parameters that minimize the objective function so that the
324 experimental and calculated TG curves match, the data obtained with the Mettler

325 Toledo TG apparatus at a $N_2:O_2 = 4:1$ atmosphere were used as initial values. The same
326 set of parameters was used in the runs carried out on the Perkin Elmer TG.

327 Table 2 shows the optimized pre-exponential factors k_{01B} obtained in each run and
328 Table 3 shows the kinetic parameters obtained for each reaction. With the optimized
329 parameters, the mass fraction curves were calculated and plotted together with their
330 experimental values, both TG and DTG, in Figures 1 to 4. The same was done in the
331 case of the other tests. It can be seen that the calculated results agree well with the
332 experimental ones in most cases (reason why the small differences cannot be observed),
333 demonstrating that the proposed model is useful for correlating the data. Figures 2c and
334 3d show the variation in volatile mass fraction for the four reactions: reactions 1A and
335 1B take place in the interval of 500-750 K, whereas reaction 2 and 3 take place in 700-
336 800 K and 750-850 K, respectively.

337 The variation coefficient of each run was calculated using a mean value for the mass
338 fraction of 0.5 in all the runs. Table 2 shows these results, where it can be seen that in
339 the $N_2:O_2 = 4:1$ runs the variations are smaller than 10 %, except in the case of the two
340 runs carried out on the Perkin Elmer TG at 5 K/min. This makes us confident about the
341 ability of our kinetic model to correlate the experimental results obtained from the two
342 different TG apparatus. It is worth noting, however, that in the two runs where the VC
343 exceeds 10 %, the experimental conversions are greater than those predicted by the
344 model, and therefore the model is useful to check that a conversion is obtained or
345 surpassed.

346 The following analysis can be done based on the obtained kinetic parameters:

347 - Reaction 1A is the most important and contributes up to 50.2 % of the initial mass,
348 whereas reaction 1B contributes only 18.7%. These two reactions have similar apparent
349 activation energies – around 125 kJ/mol – and their reaction orders are 1.73 for reaction
350 1A, and 1.07 for reaction 1B. The obtained parameters are the result of the best
351 correlation of the data, and consequently they have no clear physical meaning. This fact
352 may indicate that the proposed scheme is an over-simplification of the real process. The
353 relatively low apparent activation energy of reaction 1A and its reaction order of 1.73
354 indicate that there are many consecutive and parallel reactions giving rise to these
355 correlation values.

356 -Where reaction 1B is concerned, the vaporization effect together with consecutive and
357 parallel reactions give rise to a reaction order close to 1, a value between zero for
358 vaporization processes and orders greater than unity that can be found in literature for
359 chemical reactions. The activation energy also has a low value, but is greater than that
360 of a volatilization process (30-70 kJ/mol). It is curious that in the pyrolysis of olive oil
361 [3] using the same thermobalance, there was also a first vaporization + reaction process,
362 with a reaction order of 0.606 and an apparent activation energy of 112 kJ/mol, whereas
363 in the case of reaction 1B in the combustion process, the reaction order is 1.07 and the
364 apparent activation energy is 124 kJ/mol, a value close to 112 kJ/mol. Perhaps there is a
365 similarity between the processes of pyrolysis and combustion, with the difference being
366 that the oxidation of the reacting mass gives rise to an increase in the overall reaction
367 rate because of oxygenated radicals.

368 The kinetic parameters of reactions 1A and 1B are comparable with those (reaction
369 order around 1 and activation energy around 85-100 kJ/mol) obtained in the first step of
370 the decomposition proposed by Santos et al. [12] and also comparable to those obtained
371 by Gouveia de Souza et al. [11].

372 - For reaction 2, the apparent activation energy is high, 389 kJ/mol, and so is the
373 reaction order, 3.31. These results have opposing effects: high activation energies mean
374 sharp peaks in a DTG run, whereas high reaction orders mean broad peaks. Perhaps
375 lower activation energies and reaction orders are also acceptable. Nevertheless, the
376 obtained correlation values are optimal – also upon taking into account the other three
377 decomposition steps and all the dynamic and dynamic + isothermal runs. Gouveia de
378 Souza et al. [11] proposed activation energies of 205-300 kJ/mol and reaction orders of
379 2.0 or 2.1.

380 - Reaction 3 corresponds to the combustion of a carbonaceous residue, which is in
381 keeping with the comparison between pyrolysis and combustion runs, and considering
382 the TG-MS and TG-IR results. The activation energy and reaction order are 240 kJ/mol
383 and 1.04, respectively, which are acceptable values for combustion processes. Gouveia
384 de Souza et al. [11] proposed activation energies of 300-380 kJ/mol and reaction orders
385 of around 1.9-2.1, which are similar to those proposed by Santos et al. [12].

386 Vecchio et al [14] presented DTG data of triglycerides: tristearate, trioleate, trilinoleate
 387 and trilinolenate. They observed three steps of decomposition: a first wide one, which
 388 can be decomposed in two for trioleate, a second step with an acute peak and a third
 389 step, which corresponds to the burnout of the carbonaceous residue.

390 The data presented in Table 3 correspond to a $N_2:O_2 = 4:1$ and $N_2:O_2 = 9:1$ atmosphere.
 391 The same set of parameters was used in the correlation of runs carried out at $N_2:O_2 =$
 392 $9:1$ and $N_2:O_2 = 4:1$. However, several aspects are worth commenting:

393 - The pre-exponential factor k_{01B} of each run has been optimized, as was done in $N_2:O_2$
 394 $= 4:1$ runs.

395 - It seems that less of the carbonaceous residue forms than in the case of $N_2:O_2 = 4:1$
 396 runs, so that the mass fractions of the other reactions (1A, 1B and 2) increase, as shown
 397 in Table 3.

398 - For the runs carried out on 5 mg samples, the pre-exponential factor of reactions 1A, 2
 399 and 3 decrease with respect to $N_2:O_2 = 4:1$ runs by a factor of 0.32, which is obtained
 400 experimentally by optimization when the corresponding experimental data are
 401 correlated. This factor corresponds to a reaction order of 1.64 with respect to the oxygen
 402 partial pressure, and was calculated as follows:

$$403 \frac{\log 0.32}{\log \left[\frac{P_{O_2} \text{ for } N_2 : O_2 = 9 : 1}{P_{O_2} \text{ for } N_2 : O_2 = 4 : 1} \right]} = \frac{\log 0.32}{\log \left[\frac{0.1}{0.2} \right]} = 1.64 \quad (8)$$

404 This reaction order is greater than unity probably as a consequence of diffusion of
 405 oxygen inside the crucible, which causes the oxygen concentration in the surface of the
 406 oil to be less than the external oxygen concentration.

407 - For the runs carried out on 1 mg samples, the pre-exponential factors of reactions 2
 408 and 3 decrease by the same factor, 0.32. However, for reaction 1A, the pre-exponential
 409 factor is the same as in the $N_2:O_2 = 4:1$ run. This would indicate that in the case of
 410 reaction 1A, the oxygen is probably required as an initiator in oxygenated radical
 411 formation and as a reactant. For the runs carried out on 1 mg and 5 mg samples at $N_2:O_2$
 412 $= 4:1$, and on 1 mg at $N_2:O_2 = 9:1$, there is sufficient oxygen present to achieve the
 413 maximum degradation rate, whereas for 5 mg at $N_2:O_2 = 9:1$ there is not, and thus the

414 reaction proceeds more slowly. All these considerations highlight the complexity of the
415 process.

416 Figure 4 shows the experimental and calculated results obtained for pure olive oil, waste
417 olive oil and waste mixed oil by means of the same correlation procedure. This means
418 that approximately the same kinetic model can be applied, although for certain waste
419 mixed oils several runs should be done to confirm or modify the kinetic parameters and
420 the mass fraction of volatiles involved in each reaction.

421 The values of the pre-exponential factor k_{01B} have been correlated roughly by means of
422 a parameter P, which is defined as:

$$423 \quad P = (\text{initial mass in mg})^a \cdot (\text{heating rate in K/min})^b \cdot (\text{height in cm})^c \cdot (\text{diameter in cm})^d$$

424 The optimal values of a, b, c and d that obtain the best correlation between k_{01B} and P
425 are as follows: $a = -2.3$, $b = -0.68$, $c = -3.5$ and $d = 16.0$. A logarithmic plot of k_{01B} vs. P is
426 shown in Figure 7. The values of exponents a,b,c,d reveal a trend in the variation of
427 process 1B, when vaporization is included. If the process were only vaporization of a
428 pure substance in a pure molecular diffusion process, the expected values would be the
429 following: $a = -1$; $b = 0$; $c = -1$; $d = 2$. The obtained values differ from these, but the positive
430 and negative values follow the expected trend. The convective phenomena produced by
431 temperature gradients, the formation of small drops at the end of the run and the shape
432 of the crucible, which is not exactly cylindrical, can alter molecular diffusion inside the
433 crucible, which is one of the factors controlling the vaporization rate [20,21].

434 Figure 7

435 436 7. APPLICATION OF THE KINETIC MODEL

437 The system of equations that we have deduced is useful to characterize the
438 decomposition of olive oil, waste olive oil and more approximately the decomposition
439 of waste mixed oil. However, there are some aspects that merit consideration:

440 1. The mass fraction of the last reaction (combustion of the carbonaceous material) can
441 depend on the combustion conditions and vary between 0.13 for $N_2:O_2 = 4:1$ and 0.08
442 for $N_2:O_2 = 9:1$. For intermediate conditions, an interpolation can be done. The mass

443 fraction of the other reactions must be recalculated so that the sum of all fractions is
444 equal to unity.

445 2. The value of the pre-exponential factor k_{o1B} depends on operating conditions, so
446 extrapolation of the TG data to industrial conditions may be risky. A first approximation
447 would imply assuming that reactions 1A and 1B are similar, so that the kinetic
448 parameters of reaction 1A can be used for the sum of the mass fractions of reactions 1A
449 and 1B. An analysis of the operating conditions of the industrial process can also be
450 done to estimate the equivalent diffusion length (mass transfer coefficient/diffusivity).
451 This can be compared with the height of the crucibles that are used, in order to establish
452 whether the vaporization process implied in reaction 1B is faster or slower than reaction
453 1A. In any case, the proposed approximation may be valid.

454 8. CONCLUSIONS

455 Four decomposition steps have been suggested for correlating the complex system of
456 reactions involved in the combustion of olive oil. Reactions 1A and 1B take place at
457 500-750 K, reaction 2 at 700-800 K and reaction 3 at 750-850 K. In reaction 1B, which
458 corresponds to a vaporization + reaction process, the observed random behavior is
459 deduced to be the result of the vaporization process. The last reaction corresponds to the
460 combustion of a carbonaceous residue.

461 The obtained kinetic parameters have been instrumental to satisfactorily simulating the
462 experimental results.

463 The kinetic model might also be roughly applicable to waste olive oil and waste mixed
464 oil, although where waste mixed oil is concerned, more runs should be done to confirm
465 or vary the kinetic parameters.

466 The kinetic study carried out on different initial masses using two distinct TG apparatus
467 together with TG-MS and TG-IR data, is useful for analyzing the thermal behavior of
468 liquids and for explaining a number of random results in the TG and DTG data.

469 AUTHOR INFORMATION

470 Corresponding Author

471 *Phone: +34 96 590 35 46, Fax: +34 96 590 38 26, e-mail: rafael.font@ua.es.

472 ACKNOWLEDGMENTS

473 Support for this work was provided by PROMETEO/2009/043/FEDER of Generalitat
474 Valenciana (Spain) and CTQ2008-05520 (Spanish MCI/research).
475

Accepted Manuscript

475 REFERENCES

476

477 [1] K. D. Maher, D. C. Bressler, Pyrolysis of triglyceride materials for the production of
478 renewable fuels and chemicals, *Bioresource Technol.* 98 (2007) 2351-68.

479 [2] K. Jansson, T. Wampler, C. Zawodny, Pyrolysis GC/MS used to profile cracking
480 products of bio-oils. Technical Program- Pittcon (2007) (date: 05/09/2012;
481 http://www.analytix.co.uk/Products/Pyrolysis/CDS_pyrolysis_applications/Biofuels_Pit
482 [tcon_paper.pdf](http://www.analytix.co.uk/Products/Pyrolysis/CDS_pyrolysis_applications/Biofuels_Pittcon_paper.pdf)).

483 [3] R. Font, M.D. Rey, Kinetics of olive oil pyrolysis, *J. Anal. Appl. Pyrolysis.* 103
484 (2013) 181-188.

485 [4] A. G. D. Santos, V. P. S. Caldeira, M. F. Farias, A. S. Araújo, L.D. Souza, A. K.
486 Barros, Characterization and kinetic study of sunflower oil and biodiesel, *J. Therm.*
487 *Anal. Calorim.* 106 (2011) 747-751.

488 [5] I. M. S. Correia, M. J. B. Souza, A. S. Araújo, E. M. B. D. Sousa, Thermal stability
489 during pyrolysis of sunflower oil produced in the northeast of Brazil, *J. Therm. Anal.*
490 *Calorim.* 109 (2012) 967-974.

491 [6] A. C. R. Melo, A. S. Araujo, E.F.B. Silva, R. M. Oliveira, V. J. Fernandes Jr, G. E.
492 Luz Jr., A. G. Souza, Kinetic behavior of sunflower oil pyrolysis over mesoporous
493 materials, *Fuel Process Technol.* 92 (2011) 1340-1344.

494 [7] S. Vecchio, L. Cerretani, A. Bendini, E. Chiavaro, Thermal decomposition study of
495 monovarietal extra virgin olive oil by simultaneous thermogravimetry/differential
496 scanning calorimetry: relation with chemical composition, *J. Agric. Food Chem.* 57 (11)
497 (2009) 4793-4800.

498 [8] F. Kotti, E. Chiavaro, L. Cerretani, C. Barnaba, M. Gargouri, A. Bendini, Chemical
499 and thermal characterization of Tunisian extra virgin olive oil from Chetoui and
500 Chemlali cultivars and different geographical origin, *Eur. Food Res. Technol.* 228 (5)
501 (2009) 735-742.

502 [9] L. S. Tran, B. Sirjean, P-A Glaude, R. Fournet, F. Battin-Leclerc, Progress in
503 detailed kinetic modeling of the combustion of oxygenated components of biofuels,
504 *Energy* 43 (2012) 4-18.

505 [10] J. Dweck, C. M. S. Sampaio, Analysis of the thermal decomposition of commercial
506 vegetable oils in air by simultaneous TG/DTA, *J. Therm. Anal. Calorim.* 75 (2004) 385-
507 391.

- 508 [11] A. Gouveia de Souza, J. C. Oliveira Santos, M. M. Conceição, M. C. Dantas Silva,
509 S. Prasad, A thermoanalytic and kinetic study of sunflower oil, *Braz. J. Chem. Eng.* 21
510 (2004) 265-273.
- 511 [12] J. C. O. Santos, I. M. G. Santos, M. M. Conceição, S. L. Porto, M. F. S. Trindade,
512 A. G. Souza, S. Prasad, V. J. Fernandes Jr., A. S. Araújo, Thermoanalytical, kinetic and
513 rheological parameters of commercial edible vegetable oils, *J. Therm. Anal. Calorim.* 75
514 (2004) 419-428.
- 515 [13] X. Zhengwen, Kinetic study on pyrolysis and combustion of cooking oil tar under
516 different air concentrations by using Macro-TG-FTIR analysis, *Disaster Advances.* 5(4)
517 (2012) 1520-1524.
- 518 [14] S. Vecchio, L. Campanella, A. Nuccilli, M. Tomassetti, Kinetic study of thermal
519 breakdown of triglycerides contained in extra-virgin olive oil, *J. Therm. Anal. Calorim.*,
520 91 (2008) 51-56.
- 521 [15] M. Tomassetti, G. Favero, L. Campanella, Kinetic thermal analytical study of
522 saturated mono-, di- and tri-glycerides, *J. Therm. Anal. Calorim.*, 112 (2013) 519-527.
- 523 [16] A. K. Burnham, R. L. Braun, Global kinetic analysis of complex materials, *Energy*
524 *Fuels* 13(1) (1999) 1-22.
- 525 [17] E. Ranzi, A. Cuoci, T. Faravelli, A. Frassoldati, G. Migliavacca, S. Pierucci, S.
526 Sommariva, Chemical kinetics of biomass pyrolysis, *Energy Fuels* 22 (2008) 4292-
527 4300.
- 528 [18] J. E. White, W. J. Catallo, B. L. Legendre, Biomass pyrolysis kinetics: a
529 comparative critical review with relevant agricultural residue case studies, *J. Anal.*
530 *Appl. Pyrolysis.* 9 (2011) 1-33.
- 531 [19] M. Grønli, M.J. Antal, G. Varhegyi, A round-robin study of cellulose pyrolysis
532 kinetics by thermogravimetry, *Ind. Eng. Chem. Res.* 38 (1999) 2238-2244.
- 533 [20] R. Font, M.F. Gómez-Rico, N. Ortuño, Analysis of the vaporization process in TG
534 apparatus and its incidence in pyrolysis, *J. Anal. Appl. Pyrolysis.* 91 (2011) 89-96.
- 535 [21] R. Font, J. Moltó, N. Ortuño, Kinetics of tetrabromobisphenol A pyrolysis.
536 Comparison between correlation and mechanistic models, *J. Anal. Appl. Pyrolysis.* 94
537 (2012) 53-62.
- 538 [22] N. Vlachos, Y. Skopelitis, M. Psaroudaki, V. Konstantinidou, A. Chatzilazarou, E.
539 Tegou, Applications of Fourier transformed-infrared spectroscopy to edible oils, *Anal.*
540 *Chim. Acta* 573-574 (2006) 459-465.

- 541 [23] S. Vyazovkin, A. K. Burnham, J. M. Criado, L. A. Pérez-Maqueda, C. Popescu, N.
542 Sbirrazzuoli, ICTAC Kinetics Committee recommendations for performing kinetic
543 computations on thermal analysis data, *Thermochim. Acta* 520 (2011) 1-19.
- 544 [24] I. Martín-Gullón, M.F. Gómez-Rico, A. Fullana, R. Font, Interrelation between the
545 kinetic constant and the reaction order in pyrolysis, *J. Anal. Appl. Pyrolysis* 68-69
546 (2003) 645-655.
- 547
548

Accepted Manuscript

548 LIST OF TABLES

549

550 **Table 1.** Elemental analysis of the samples.

551

552 **Table 2.** Operating conditions and values of k_{o1B}

553

554 **Table 3.** Kinetic parameters for a $N_2:O_2 = 4:1$ and a $N_2:O_2 = 9:1$ atmosphere.

555 FIGURE LEGENDS

556 **Figure 1.** Variation of weight fraction vs. temperature for runs carried out on different
557 initial masses of pure olive oil at different heating rates.

558

559 **Figure 2.** Variation of weight fraction vs. temperature for runs carried out on 5 mg of
560 pure olive oil at different heating rates (in Figure 2c: 1A, 1B, 2 and 3 is the weight
561 fraction of volatiles evolved in reactions 1A, 1B, 2 and 3).

562

563 **Figure 3.** Variation of weight fraction vs. temperature for runs carried out on 1 mg of
564 pure olive oil at different heating rates (in Figure 3d: 1A, 1B, 2 and 3 is the weight
565 fraction of volatiles evolved in reactions 1A, 1B, 2 and 3).

566

567 **Figure 4.** Variation of weight fraction vs. temperature for pure olive oil and waste oils.

568

569 **Figure 5.** Variation of mass fraction and evolution of gases detected in the TG-MS run
570 carried out on pure olive oil.

571

572 **Figure 6.** IR spectrum of the gases and volatiles evolved in a TG-IR run.

573

574 **Figure 7.** Variation of k_{o1B} vs. parameter P.

575

576

577

A kinetic model, including vaporization and reaction, is proposed

Two TG apparatus have been used, so the results can be compared

The kinetic model is supported by TG-MS and TG-IR runs.

Accepted Manuscript

| | Carbon (%) | Hydrogen (%) | Oxygen (%) | Nitrogen (%) | Sulfur (%) | Net calorific value (kcal/kg) |
|------------------------|-------------------|---------------------|-------------------|---------------------|-------------------|--------------------------------------|
| Olive oil | 77.5 | 11.6 | 10.9 | 0.0 | 0.0 | 8884 |
| Waste olive oil | 77.2 | 11.6 | 11.2 | 0.0 | 0.0 | 8859 |
| Waste Mixed oil | 76.9 | 11.6 | 11.5 | 0.0 | 0.0 | 8784 |

Accepted Manuscript

| | $N_2:O_2$ ratio | M (mg) | Run | Heating rate (K/min) | TG Apparatus | Crucible Material | Height (cm) | Int. Diam. (cm) | k_{01B} (s^{-1}) | Parameter P | VC (%) |
|-----------------|--------------------|--------|-------|-------------------------|----------------|----------------------|----------------|--------------------|------------------------|----------------------|-----------|
| Olive oil | 4 : 1 | 4.791 | D | 20 | Mettler Toledo | Aluminium | 0.41 | 0.55 | $7.324 \cdot 10^8$ | $2.18 \cdot 10^{-7}$ | 4.1 |
| Waste olive oil | 4 : 1 | 6.187 | D | 20 | Mettler Toledo | Alumina | 0.425 | 0.47 | $3.481 \cdot 10^7$ | $1.56 \cdot 10^{-7}$ | 7.1 |
| Waste mixed oil | 4 : 1 | 5.643 | D | 20 | Mettler Toledo | Alumina | 0.425 | 0.47 | $1.361 \cdot 10^7$ | $1.96 \cdot 10^{-7}$ | 7.9 |
| Olive oil | 4 : 1 | 5.024 | D | 10 | Mettler Toledo | Aluminium | 0.41 | 0.55 | $1.354 \cdot 10^7$ | $2.19 \cdot 10^{-7}$ | 4.1 |
| Waste olive oil | 4 : 1 | 5.020 | D | 10 | Mettler Toledo | Aluminium | 0.41 | 0.55 | $2.513 \cdot 10^7$ | $2.19 \cdot 10^{-7}$ | 4.7 |
| Olive oil | 4 : 1 | 4.996 | D | 10 | Mettler Toledo | Aluminium | 0.41 | 0.55 | $2.468 \cdot 10^7$ | $2.22 \cdot 10^{-7}$ | 4.7 |
| Olive oil | 4 : 1 | 5.242 | D | 5 | Mettler Toledo | Aluminium | 0.41 | 0.55 | $7.257 \cdot 10^7$ | $2.22 \cdot 10^{-7}$ | 5.1 |
| Olive oil | 4 : 1 | 1.120 | D | 20 | Mettler Toledo | Aluminium | 0.41 | 0.55 | $4.682 \cdot 10^9$ | $7.96 \cdot 10^{-6}$ | 4.7 |
| Olive oil | 4 : 1 | 1.095 | D | 10 | Mettler Toledo | Aluminium | 0.41 | 0.55 | $5.945 \cdot 10^9$ | $9.49 \cdot 10^{-6}$ | 7.2 |
| Olive oil | 4 : 1 | 1.047 | D | 5 | Mettler Toledo | Aluminium | 0.41 | 0.55 | $7.508 \cdot 10^9$ | $1.20 \cdot 10^{-5}$ | 6.9 |
| Olive oil | 4 : 1 | 5.025 | D + I | 10 | Mettler Toledo | Aluminium | 0.41 | 0.55 | $2.709 \cdot 10^7$ | $2.18 \cdot 10^{-7}$ | 4.8 |
| Olive oil | air | 5.205 | D | 20 | Perkin Elmer | Alumina | 0.645 | 0.42 | $1.104 \cdot 10^{10}$ | $4.29 \cdot 10^{-5}$ | 9.3 |
| Olive oil | air | 5.051 | D | 10 | Perkin Elmer | Alumina | 0.645 | 0.42 | $5.418 \cdot 10^9$ | $5.21 \cdot 10^{-5}$ | 6.8 |
| Olive oil | air | 5.138 | D | 5 | Perkin Elmer | Alumina | 0.645 | 0.42 | $1.889 \cdot 10^{10}$ | $5.63 \cdot 10^{-5}$ | 19.3 |
| Olive oil | air | 10.096 | D | 20 | Perkin Elmer | Alumina | 0.645 | 0.42 | $8.099 \cdot 10^8$ | $8.32 \cdot 10^{-6}$ | 4.4 |
| Olive oil | air | 10.808 | D | 10 | Perkin Elmer | Alumina | 0.645 | 0.42 | $1.788 \cdot 10^8$ | $7.92 \cdot 10^{-6}$ | 7.5 |
| Olive oil | air | 10.855 | D | 5 | Perkin Elmer | Alumina | 0.645 | 0.42 | $7.504 \cdot 10^9$ | $8.83 \cdot 10^{-6}$ | 7.7 |
| Olive oil | air | 10.115 | D + I | 20 | Perkin Elmer | Alumina | 0.645 | 0.42 | $7.804 \cdot 10^8$ | $8.28 \cdot 10^{-6}$ | 2.9 |
| Olive oil | air | 10.966 | D + I | 10 | Perkin Elmer | Alumina | 0.645 | 0.42 | $7.466 \cdot 10^9$ | $7.64 \cdot 10^{-6}$ | 8.8 |
| Olive oil | air | 5.152 | D + I | 5 | Perkin Elmer | Alumina | 0.645 | 0.42 | $4.058 \cdot 10^{10}$ | $5.59 \cdot 10^{-5}$ | 21.5 |
| Olive oil | 9 : 1 | 5.081 | D | 20 | Mettler Toledo | Aluminium | 0.41 | 0.55 | $5.728 \cdot 10^7$ | $1.89 \cdot 10^{-7}$ | 8.5 |
| Olive oil | 9 : 1 | 5.006 | D | 10 | Mettler Toledo | Aluminium | 0.41 | 0.55 | $4.634 \cdot 10^7$ | $2.20 \cdot 10^{-7}$ | 4.2 |
| Olive oil | 9 : 1 | 4.954 | D | 5 | Mettler Toledo | Aluminium | 0.41 | 0.55 | $4.237 \cdot 10^7$ | $2.55 \cdot 10^{-7}$ | 3.9 |
| Olive oil | 9 : 1 | 1.113 | D | 20 | Mettler Toledo | Aluminium | 0.41 | 0.55 | $1.300 \cdot 10^8$ | $8.09 \cdot 10^{-6}$ | 9.3 |
| Olive oil | 9 : 1 | 1.062 | D | 10 | Mettler Toledo | Aluminium | 0.41 | 0.55 | $1.273 \cdot 10^8$ | $1.02 \cdot 10^{-5}$ | 4.9 |
| Olive oil | 9 : 1 | 1.156 | D | 5 | Mettler Toledo | Aluminium | 0.41 | 0.55 | $2.781 \cdot 10^9$ | $9.35 \cdot 10^{-6}$ | 14.0 |

| Reaction | Temperature Interval (K) | k_{i0} (s^{-1}) for $N_2:O_2 = 4:1$ and air | k_{i0} (s^{-1}) for $N_2:O_2 = 9:1$ | E_i (kJ/mol) | n_i | $v_{i\infty}$ for $N_2:O_2 = 4:1$ | $v_{i\infty}$ for $N_2:O_2 = 9:1$ |
|-----------|---|---|---|-------------------|-------|--------------------------------------|--------------------------------------|
| 1A | 520-700 | $5.979 \cdot 10^8$ | $0.32 \cdot 5.979 \cdot 10^8$ (for 5 mg initial mass) $5.979 \cdot 10^8$ (for 1 mg initial mass) | 127.3 | 1.73 | 0.502 | 0.532 |
| 1B | 500-750 (depending on operating conditions) | see Table 2 | see Table 2 | 124.2 | 1.07 | 0.187 | 0.198 |
| 2 | 700-800 | $3.788 \cdot 10^{27}$ | $0.32 \cdot 3.788 \cdot 10^{27}$ | 389.3 | 3.31 | 0.178 | 0.188 |
| 3 | 750-850 | $5.040 \cdot 10^{13}$ | $0.32 \cdot 5.040 \cdot 10^{13}$ | 240.7 | 1.08 | 0.132 | 0.080 |

